phys. stat. sol. (a) 54, 171 (1979)

Subject classification: 11; 10.1; 21

School of Engineering and Applied Science, University of California, Los Angeles[1])

The Simultaneous Clustering of Point Defects during Irradiation

By
N. M. GHONIEM and D. D. CHO

The simultaneous clustering of irradiation produced vacancies and interstitials in metals is investigated using the rate theory approach. Rate equations are used to describe the time-dependent concentrations of point defect clusters. Size-dependent bias factors and self-consistent reaction rate constants are used to evaluate the feed-back effects between the evolving vacancy cluster and interstitial loop populations. It is found that the concurrent presence of vacancy clusters depletes the free vacancy population and thereby reduces mutual point defect recombination. This has the effect of enhancing interstitial loop formation; increasing loop concentration, nucleation rate, average size, and growth speed of the average size. In 316 stainless steel, a diinterstitial binding energy of 1.19 eV results in a substantial decrease in loop concentrations at high temperatures, which is in qualitative agreement with experimental data.

Es wird die gleichzeitige Clusterbildung von durch Strahlung erzeugten Leerstellen und Zwischengitterstörstellen mit der Methode der Ratengleichungen untersucht. Bilanzgleichungen werden benutzt, um die zeitabhängigen Konzentrationen der Punktdefektcluster zu beschreiben. Größenabhängige Vorfaktoren und selbstkonsistente Reaktionskonstanten werden benutz, um die Rückkopplungseffekte zwischen den sich entwickelnden Leerstellencluster und den Besetzungen der Interstitialschleifen zu berechnen. Es wird gefunden, daß die konkurrierende Anwesenheit von Leerstellencluster die Besetzung freier Leerstellen verringert und dabei die gegenseitige Punktdefektrekombination verringert. Dies führt zu einer Erhöhung der Zwischengitterschleifenbildung und vergrößert die Schleifenkonzentration, Keimbildungsrate, mittlere Größe und die Wachstumsgeschwindigkeit der mittleren Ausdehnung. In rostfreiem 316-Stahl führt eine Bindungsenergie von 1,19 eV der Di-Interstitials zu einer beträchtlichen Verringerung der Schleifenkonzentration bei hohen Temperaturen, die in qualitati er Übereinstimmung mit experimentellen Ergebnissen ist.

1. Introduction

It has become important to investigate the detailed effects of material and irradiation variables on the nucleation and growth of interstitial loops. Recently, Johnson [1] showed that the diinterstitial binding energy has a significant influence on the formation of interstitial loops in metals irradiated at high temperatures. On the other hand, Hall and Potter [2] examined the kinetics of interstitial loop nucleation and growth during low dose irradiation, paying special attention to impurity and trapping effects.

The aim of the present paper is to give an understanding of the coupling between simultaneously forming vacancy and interstitial clusters during irradiation. The salient features of the investigation are summarized as: (1) size-dependent bias factors for point defect diffusion to interstitial loops and microvoids are used to calculate reaction rates, (2) mixed rate reactions (diffusion and surface limited) are assumed for the computation of point defect impingement and emission fluxes, (3) point defect conservation equations are utilized to determine the necessary number of rate equations at any irradiation time, (4) the relationship between vacancy and interstitial cluster formation is analyzed.

[1]) Los Angeles, California 90024, USA.

14

2. A Model for the Simultaneous Formation of Defect Clusters

2.1 Rate constants

In the *jump* method [3], the reaction between diffusing species proceeds by a surface control mechanism. On the other hand, the rate constants in the *diffusion* method are obtained by solving steady-state diffusion equations [3]. Defining the instability radius of a particular cluster, R, as the radius at which point defects will inevitably be attracted towards the cluster (interaction energy $\approx kT$), then

$$R = Z(r)\, r\,, \tag{1}$$

where r is the physical cluster radius and $Z(r)$ is a size-dependent bias factor (capture efficiency). Results of the detailed elasticity calculations of Wolfer and Ashkin [4] have been used in (1). The overall reaction rate constant is obtained in a manner similar to that used to determine the overall heat flux with series resistance [5].

Define x as the cluster size in atomic units, i for an interstitial, v for a vacancy, l for a loop, and c for a cavity. For a spherical cluster in f.c.c. lattices the following impingement frequencies, K (s^{-1}), are used:

$$K^{c}_{v,i}(x) = \frac{2.216[Z^{c}_{v,i}(x)]^2\, x^{2/3}}{1 + 0.1128 Z^{c}_{v,i}(x)\, x^{1/3}}\, \nu_{v,i}\, \exp\left(\frac{-E^{m}_{v,i}}{kT}\right), \tag{2}$$

where ν is the atomic vibrational frequency, $E^{m}_{v,i}$ the vacancy–interstitial migration energy, k the Boltzmann constant, and T the absolute irradiation temperature. For large size cavities the reaction rate is purely diffusion controlled and the impingement frequency is proportional to $x^{1/3}$. Interstitial clusters are treated as small spherical inclusions with the application of (2) up to a maximum size x_i^{max} of few interstitials. However, larger sizes behave as two-dimensional disks and the interaction with point defects is only surface controlled. The relevant impingement frequency is thend

$$K^{l}_{v,i}(x) = 1.555 Z^{l}_{v,i}(x)\, x^{1/2} \nu_{v,i} \exp\left(\frac{-E^{m}_{v,i}}{kT}\right). \tag{3}$$

The emission of vacancies from the surface of vacancy clusters is included in this model. However, point defect thermal emission from interstitial loops is not considered because of the small probability of this process for small size loops. The only thermal dissociation process treated is that for diinterstitial break-up. The emission *rate* of vacancies from a vacancy cluster size x is given by

$$\gamma^{e}_{v}(x) = K^{c}_{v}(x)\, C^{e}_{v} \exp\left[\left(\frac{1.28 g a^2}{kT}\right) x^{-1/3}\right], \tag{4}$$

where a (cm) is the lattice constant, g (eV/cm^2) the surface energy, and C^{e}_{v} is the thermal matrix fractional vacancy concentration. Diinterstitial and divacancy thermal dissociation rates are given as

$$\gamma^{c,l}_{v,i}(2) = K^{c,l}_{v,i}(2) \exp\left(-\frac{E^{B}_{2v,2i}}{kT}\right), \tag{5}$$

where E^{B}_{2v} and E^{B}_{2i} are the binding energies for divacancies and diinterstitials, respectively.

2.2 Rate Equations

In this section, a set of rate equations is used to describe the nucleation and growth of both voids and interstitial loops. Using the assumptions homogeneous rate theory, and the nomenclature of chemical kinetics, one can write the following set of

equations for the fractional concentrations:

$$
\left.
\begin{aligned}
&\frac{dC_v}{dt} = P + K_i^c(2)\, C_i C_{2v} + \left(2\gamma_v^c(2) - K_v^c(2)\, C_v\right) C_{2v} + \\
&\quad + \sum_{x=3}^{x_{max}} \left(\gamma_v^c(x) - K_v^c(x)\, C_v\right) C_{xv} - \sum_{x=3}^{x_{max}} K_v^l(x)\, C_v C_{xi} + \\
&\quad + Z_v \varrho_d D_v (C_v^e - C_v) - \alpha C_v C_i - K_v^c(1)\, C_v^2 - K_v^l(2)\, C_v C_{2i}\,, \\
&\frac{dC_{2v}}{dt} = \frac{1}{2} K_v^c(1)\, C_v^2 + \gamma_v^c(3)\, C_{3v} + K_i^c(3)\, C_i C_{3v} + \varrho_d D_{2v} C_{2v}^e - \\
&\quad - K_v^c(2)\, C_v C_{2v} - K_i^c(2)\, C_i C_{2v} - \gamma_v^c(2)\, C_{2v} - \varrho_d D_{2v} C_{2v}\,, \\
&\vdots \\
&\frac{dC_c(x)}{dt} = K_v^c(x-1)\, C_v C_c(x-1) - \left[K_i^c(x)\, C_i + K_v^c(x)\, C_v + \right. \\
&\quad \left. + \gamma_v^c(x)\right] C(x) + \left[K_i^c(x+1)\, C_i + \gamma_v^c(x+1)\right] C_c(x+1)\,, \\
&\frac{dC_i}{dt} = P + K_v^l(2)\, C_v C_{2i} - K_v^c(1)\, C_i^2 - \alpha C_v C_i - \\
&\quad - K_i^l(2)\, C_i C_{2i} - K_i^c(2)\, C_i C_{2v} - \sum_{x=3}^{x_{max}} K_i^l(x)\, C_i C_{xi} - \\
&\quad - \sum_{x=3}^{x_{max}} K_v^c(x)\, C_i C_{xv} - Z_i \varrho_d D_i C_i\,, \\
&\frac{dC_{2i}}{dt} = \frac{1}{2} K_i^l(2)\, C_i^2 + K_v^l(3)\, C_v C_{3i} - K_i^l(2)\, C_i C_{2i} - K_v^l(2)\, C_v C_{2i}\,, \\
&\vdots \\
&\frac{dC_l(x)}{dt} = K_i^l(x-1)\, C_i C_i(x-1) + \gamma_v^l(x-1)\, C_l(x-1) - \\
&\quad - \left\{K_i^l(x)\, C_i + K_v^l(x)\, C_v + \gamma_v^l(x)\right\} C_l(x) + \\
&\quad + K_v^l(x+1)\, C_v C_l(x+1)
\end{aligned}
\right\} \quad (6)
$$

with the parameters defined as P (at/at/s) irradiation production rate of Frenkel pairs, α (s^{-1}) point defect recombination coefficient,

$$\alpha = 48 \nu_i \exp\left(-\frac{E_i^m}{kT}\right), \quad (7)$$

$Z_{v,i}$ point defect–straight dislocation bias factors, ϱ_d (cm^{-2}) straight dislocation density, $D_{v,i}$ ($cm^{-2}\,s^{-1}$) point defect diffusion coefficients, D_{2v} ($cm^{-2}\,s^{-1}$) divacancy diffusion coefficient [6],

$$D_{2v} = \nu_v a^2 \exp\left(-\frac{E_m^{2v}}{kT}\right), \quad (8)$$

E_m^{2v} migration energy of a divacancy and C_{2v}^e (at/at/s) divacancy thermal fractional concentration [6],

$$C_{2v}^e = 6 \exp\left(-\frac{2E_F^v - E_B^{2v}}{kT}\right). \quad (9)$$

The set of rate equations (6) are derived by considering the balance between various production and destruction processes for a certain cluster size. A detailed description of this derivation is given in [7]. The analytical solution of this set of equations can be very complicated, and would have to involve numerous approximations, therefore a numerical approach is followed.

3. Method of Solution

Two distinct problems arise when one attempts to numerically solve a large number of coupled rate equations such as that described in the previous section. The first complication is due to the time scales of the problem while the second stems from handling a large set of equations. Some reaction rates are very fast while others are very slow giving rise to a stiff system of ordinary differential equations. For stability requirements, most of the conventional methods limit the integration time step to small values. This can considerably increase the computing time, and is impractical for solving our system. On the other hand, storage requirements can seriously discourage handling large systems of equations. Fortunately, the Gear [8] computer package was designed to handle both large and stiff systems of ordinary differential equations (ODEs).

The rate equations described in the previous section have been numerically integrated using the GEAR computer package. Up to 200 rate equations were solved with no storage problems on the IBM 360/90 computer. On the other hand, a total of 178 CPU seconds were required to integrate 100 rate equations simultating the irradiation behavior of 316 stainless steel at 450 °C, a dose rate of 10^{-6} dpa/s and a dislocation density of 10^9 cm/cm^3.

The total number of rate equations required to give information on the system has been arbitrarily chosen by various investigators [1, 2, 9]. In this work, we use a conservation principle for irradiation produced defects to determine the necessary number of equations. For interstitial clusters, and at any irradiation time t^*, the integrated rate of interstitial accumulation should be equal to the total number of interstitials in loops; or,

$$\left| \sum_{x=2}^{N} \left\{ \int_0^{t^*} [K_i^1(x-1,t')\, C_i(t') - K_v^1(x,t')\, C_v(t')]\, C_1(x,t)\, dt' - x C_1(x,t^*) \right\} \right| \leqq \varepsilon', \quad (10)$$

where ε' is an absolute error. Dividing by the total number of interstitials in loops $\left(f(t^*) \equiv \sum_{x=2}^{N} x C_1(x, t^*)\right)$, one gets

$$\left| \frac{1}{f(t^*)} \int_0^{t^*} \left\{ \sum_{x=2}^{N} [K_i^1(x-1, t')\, C_i(t') - K_v^1(x, t')\, C_v(t')]\, C_1(x, t') \right\} dt' - 1 \right| \leqq \varepsilon, \quad (11)$$

where ε is a relative error. Here, the number of necessary equations, N, is determined at any time t^* such that the relative error in (11) is typically small.

4. Result and Discussion

4.1 Analysis of a reference case

Many material and irradiation variables can affect the clustering kinetics of both interstitial loops and voids. For practical considerations, however, 316 stainless steel irradiated in fusion reactor first wall environment will be considered. In addition to the material parameters of Table 1, the following input parameters are adopted fot

Table 1
Model input parameters for 316 stainless steel

parameter	symbol	numerical value	units	ref.
interstitial-interstitial combinatorial number	$C_i(1)$	84		[9]
vacancy–vacancy combinatorial number	$C_v^c(1)$	84		[9]
vacancy migration energy	E_v^m	1.4	eV	[11]
interstitial migration energy	E_i^m	0.2	eV	[11]
vacancy formation energy	E_v^f	1.6	eV	[11]
interstitial formation energy	E^f_i	4.08	eV	[11]
lattice parameter	a	3.63	Å	[9]
interstitial frequency	ν_i	5×10^{12}	s^{-1}	[1]
vacancy frequency	ν_v	5×10^{13}	s^{-1}	[1]
divacancy migration energy	E_{2v}^M	0.9	eV	[6]
divacancy binding energy	E_{2v}^B	0.25	eV	[6]
trivacancy binding energy	E_{3v}^B	0.76	eV	[6]
vacancy–dislocation bias factor	Z_v	1.0		[11]
interstitial–dislocation bias factor	Z_i	1.08		[11]
surface energy	g	6.24×10^{14}	eV/cm^2	[11]

the analysis of this reference case: irradiation temperature 450 °C, initial dislocation density 10^9 cm/cm^3, dose rate 10^{-6} dpa/s.

First, we consider the evolution of interstitial clusters under these conditions with only single vacancies and interstitial loops allowed to exist, and then the effects of simultaneously forming microvoids will be explored.

Fig. 1 depicts the general characteristics of the clustering process at 450 °C. During the early stages of irradiation (times $\leqq 10\,\mu s$) the vacancy concentration remains around the thermodynamic equilibrium value ($\approx 7 \times 10^{-12}$ at/at) while the interstitial concentration builds up linearly with time. Point defects accumulate in the matrix, since no major loss mechanism is active yet. Between 10 μs and 1 ms, the interstitial concentration levels off and then decreases, due to the fast diffusion of interstitials to straight dislocations. However, single vacancies keep on accumulating in the matrix as a result of their low diffusion rate. Single interstitials are mainly removed by diffusion to straight dislocations and by mutual recombination with vacancies. Diffusion to straight dislocations is the major removal process at the start.

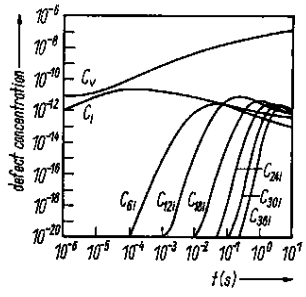

Fig. 1. Interstitial loop fractional concentrations as functions of irradiation time in the absence of microvoids. $T = 450$ °C, $\varrho_d = 10^9$ cm/cm^3, dose rate 10^{-6} dpa/s

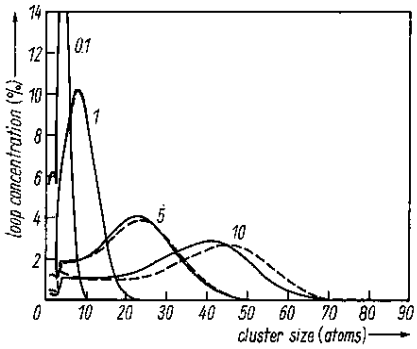

Fig. 2. Interstitial loop size distributions at various irradiation times. ——— without vacancy clusters, - - - - with vacancy clusters. $T = 450$ °C, $\varrho_d = 10^9$ cm/cm^3, dose rate 10^{-6} dpa/s

of irradiation, and then recombination dominates at longer times. For example, at 5 ms, about 50% of interstitials recombine, 49.3% are absorbed at straight dislocations, and 0.8% contribute to the formation of interstitial clusters. It is observed from Fig. 1 that the drop in the single interstitial concentration is in keeping with a loss rate of $\approx 100.1\%$. The loss rate greater than 100% of the production rate indicates a continuous bleeding from matrix interstitial inventory, contributing to the evolution of larger size clusters. Smaller clusters start to linearly accumulate at short times, then larger sizes grow on the expense of the small size clusters. This process leads to concentration maxima of ever increasing larger sizes as irradiation proceeds.

When microvoids are included, the general trends remain the same as described above. However, the magnitude of characterizing quantities change. Ten equations representing vacancy clusters were numerically solved with up to 190 equations for interstitial loops. Only ten equations were necessary for vacancy clusters because the irriadiation times considered in this work are too short to allow larger vacancy cluster formation. The interstitial size distribution, at different irradiation times, is shown in Fig. 2 for the two cases investigated here. It can be seen that including vacancy clusters has considerable effects on the size distribution, especially for longer irradiation periods. Results of the calculations indicate that larger loops grow faster in the presence of microvoids. Consequently, a broader size distribution is created when vacancy clusters are included.

Due to a larger sink density in the presence of microvoids, one might intuitively expect slower growth kinetics of interstitial loops. On the contrary, when microvoids are included, the nucleation rate and average growth speed are significantly enhanced. The presence of microvoids reduces the free vacancy concentration, thus reducing matrix point defect recombination and increasing free interstitial concentration. This will tend to promote interstitial loop nucleation increasing average growth speed, average loop size, nucleation rate, and total loop concentration, as can be seen from Table 2.

4.2 Effect of initial dislocation density

The calculations indicate that a broader interstitial loop distribution is produced when the initial dislocation density is lowered to 10^8 cm/cm^3. On the contrary, slower growth kinetics are associated with high dislocation densities resulting in a narrower loop distribution. An important result of the computations is that interstitial loop formation has distinct transient and steady state regimes. Linear loop accumulation starts 5 to 10 s after the beginning of irradiation, as can be observed from Fig. 3. The same figure shows that the total loop concentration is roughly inversely proportional to the initial dislocation density. On the other hand, the average loop size and its growth speed have been found to increase as the initial dislocation density decreases.

Table 2

Comparison of the reference case with and without microvoids after 10 s of irradiation for 316 stainless steel at 450 °C, $\varrho_d = 10^9$ cm/cm³ and 10^{-6} dpa/s

parameter	with microvoids	without microvoids	% change
vacancy concentration (at/at)	1.718×10^{-7}	2.1891×10^{-7}	−21.5
interstitial concentration at/at()	5.926×10^{-13}	4.665×10^{-13}	+27.0
average loop size (at)	37.13	34.63	+ 7.2
growth speed (at/s)	2.82	2.35	+20.0
nucleation rate (loops/cm³/s)	2.5×10^{11}	1.58×10^{11}	+37.2
total loop concentration (loops/cm³)	1.42×10^{13}	1.36×10^{13}	+4.6

4.3 Diinterstitial binding energy effect

Previous theoretical investigations [9] of interstitial loop formation and growth assumed that diinterstitial binding energy is so large that once they form, diinterstitials will never break up to single interstitials. Recently, Johnson [1] studied the effect of diinterstitial binding on *small* interstitial loops. In this section, we investigate diinterstitial binding energy effects on clusters of sizes up to 190 interstitials.

Total loop concentrations as a function of irradiation time are shown in Fig. 4 for $E_{2i}^B = 0.76$, 1.19, 1.5, and $\geqq 2.0$ eV. It is interesting to note that binding energies $\geqq 2$ eV will give identical results, indicating that $E_{2i}^B = 2$ eV is just as strong as any arger binding energy at 450 °C. It is also clear that E_{2i}^B has a dramatic effect on the

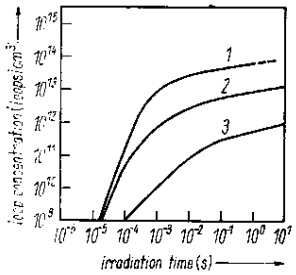

Fig. 3

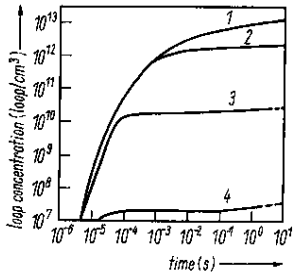

Fig. 4

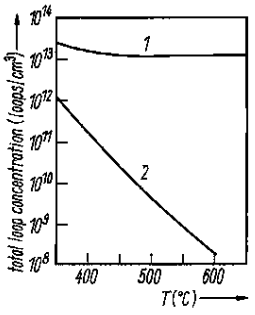

Fig. 5

Fig. 3. Effect of initial dislocation density on the total loop concentration. (1) $\varrho_d = 10^8$, (2) 10^9, (3) 10^{10} cm/cm³. $T = 450$ °C, dose rate 10^{-6} dpa/s

Fig. 4. Effect of diinterstitial binding energy on the total loop concentration. (1) $E_{2i}^B \geqq 2.0$ eV, (2) $E_{2i}^B = 1.5$, (3) 1.19, and (4) 0.76 eV

Fig. 5. Total loop concentration as a function of irradiation temperature. (1) $E_{2i}^B \geqq 2.0$ eV, (2) $E_{2i}^B = 1.19$ eV

total interstitial loop population, which becomes large for high binding energies and small for low binding energies.

4.4 Temperature dependence

The temperature dependence of interstitial loop clustering has been studied using the model parameters and a dislocation density of 10^9 cm/cm^3 at 10^{-6} dpa/s. Total interstitial loop concentration is shown in Fig. 5 as a function of temperature for $E_{2i}^B = 1.19$ eV and $\geqq 2$ eV. For $E_{2i}^B \geqq 2$ eV., the interstitial loop concentration is large and insensitive to the irradiation temperature. However, a smaller diinterstitial binding energy ($E_{2i}^B = 1.19$ eV) has the effect of a sharp drop in loop concentrations at higher temperatures. This behavior has been experimentally observed [10].

5. Conclusions

The detailed rate theory model presented in this paper has indicated that the total interstitial loop concentration is reduced when vacancy clustering is simultaneously taken into consideration. This is found to be due to a higher free interstitial concentration which results from a small recombination rate with free vacancies. It is shown that the total interstitial loop concentration will increase almost linearly with irradiation dose after an initial transient. It is also concluded that the nucleation rate, growth speed, and average size of interstitial loops are all enhanced by the simultaneous microvoid formation.

High initial dislocation density has been found to considerably slow down the kinetics of interstitial loop formation. The large sink strength of straight dislocations reduces matrix point defect fluxes. This constricts the formation of interstitial loops reducing their total concentration, average size, and growth speed.

Studying the diinterstitial binding energy effects on the temperature dependence of interstitial loop concentrations revealed that a binding energy of 1.19 eV results in lowering the total interstitial loop concentration at high temperatures due to diinterstitial dissociation.

Acknowledgement

This work was supported by the National Science Foundation through Grant No. ENG78-05413.

References

[1] R. A. JOHNSON, J. nuclear Mater. (Amsterdam) 75, 77 (1978).
[2] B. O. HALL and D. I. POTTER, Proc. IX. Internat. Symp. Eff. Rad. Structural Mat., Richland, WA 1978.
[3] U. GOSELE, J. nuclear Mater. (Amsterdam) 78, 83 (1978).
[4] W. G. WOLFER and M. ASHKIN, J. appl. Phys. 46, 547 (1975).
[5] D. R. OLANDER, Fundamental Aspects of Nuclear Fuel Elements, NTIS publication, Tennesse 1976 (p. 215).
[6] A. C. DAMASK and G. DIENES, Phys. Rev. 120, 99 (1960).
[7] N. M. GHONIEM and D. D. CHO, Univ. Calif. Eng. Rep., UCLA-ENG-7845, Los Angeles 1978.
[8] A. C. HINDMARCH, Lawrence Livermore Lab. Rep., UCID-30001, Rev. 3, Livermore 1974.
[9] M. R. HAYNS, J. nuclear Mater. (Amsterdam) 56, 267 (1975).
[10] H. R. BRAGER and J. L. STRAALSUND, J. nuclear Mater. (Amsterdam) 46, 134 (1973).
[11] N. M. GHONIEM and G. L. KULCINSKI, Radiat. Eff., in the press.

(Received March 7, 1979)